# Amorphous Calcium–Magnesium Carbonate (ACMC) Accelerates Dolomitization at Room Temperature under Abiotic Conditions

German Montes-Hernandez, François Renard, Anne-Line Auzende, Nathaniel Findling

# Amorphous calcium-magnesium carbonate (ACMC) accelerates dolomitization at room temperature under abiotic conditions

German Montes-Hernandez[a] *, François Renard[a, b], Anne-Line Auzende[a], Nathaniel Findling[a]

[a] Univ. Grenoble Alpes, Univ. Savoie Mont Blanc, CNRS, IRD, IFSTTAR, ISTerre, 38000 Grenoble, France

[b] The Njord Centre, Department of Geosciences, University of Oslo, box 1048 Blindern, 0316 Oslo, Norway

*Corresponding author: Dr. German Montes-Hernandez

E-mail address: german.montes-hernandez@univ-grenoble-alpes.fr

## Abstract

The challenge to produce dolomite $CaMg(CO_3)_2$ at low temperature (20-35°C) over laboratory time scales remains so far unsuccessful, which has led to long-lasting scientific debates in the last two centuries. This mineral exerts a major control on the natural carbon dioxide sequestration into various sedimentary, basaltic and mantellic rocks. The present study reports on specific abiotic conditions that allows the precipitation of disordered dolomite, high Mg-calcite and high Ca-magnesite at room temperature over time scales of hours to days. Here we show that an amorphous calcium magnesium carbonate (ACMC) phase accelerates dolomitization at room temperature. ACMC is initially precipitated by mixing a carbonate ($HCO_3^-/CO_3^{2-}=1$; $pH \sim 10.3 \sim pK_{a2}$) alkaline solution with a Mg-Ca ionic solution (Mg molar fraction between 0 and 1). Then, time-resolved in situ Raman spectroscopy monitored the transformation of ACMC into Mg-rich carbonate minerals. The initial Mg molar fraction controlled both the reaction mechanism (e.g. nature of transient crystalline phases) and the kinetics. Nanosized crystallites with short-range order, called disordered dolomite $CaMg(CO_3)_2$, precipitated following a complex reaction pathway. Firstly, nesquehonite ($MgCO_3.3H_2O$: nucleation time = 2.5h), then disordered dolomite ($CaMg(CO_3)_2$: nucleation time = 3.2h) and then monohydrocalcite ($CaCO_3.H_2O$: nucleation time = 3.4h) formed from ACMC transformation. Nesquehonite and monohydrocalcite are transient phases that nourish the slow precipitation of disordered dolomite, which reached a spectral equilibrium after 7 days of reaction. Direct transformation of ACMC into disordered dolomite was also measured. Our experimental results demonstrate that disordered dolomite precipitates at room temperature when ideal Mg/Ca ratio, high-carbonate alkalinity and high ionic-concentration are reached in abiotic systems. This result suggests the possibility of a physicochemical rather than to biotic control on the formation

of disordered dolomite at low temperature in several geosystems.

**Keywords:** Disordered dolomite, Mg-carbonate, Amorphous carbonate; Time-resolved Raman spectroscopy; Mineral nucleation and growth

## 1. Introduction

Dolomite, $CaMg(CO_3)_2$, precipitation kinetics and formation mechanism have been widely studied and controversial claims have been reported in the past two centuries (1). Abiotic precipitation of dolomite at ambient temperature (~25°C) is virtually impossible within typical laboratory experimental time scales (2-5). This difficulty is interpreted to originate from the strongly bonded solvation shells of magnesium ions into aqueous media (2). Dehydration of Mg ions is significantly facilitated by bacterial activity, including exopolymeric substances, and organic functionalized surfaces (6-7). Therefore, several studies have claimed that dolomite may precipitate in bio-assisted systems at ambient laboratory conditions (6-12). Therefore, both textural and crystallographic characterization, reaction mechanism, and kinetics studies of dolomite precipitation at ambient/low temperature remain exciting scientific challenges for geochemists and mineralogists (13-17).

In addition, the effect of Mg hydration might not be the only factor of inhibition of dolomite formation at room temperature. Recent studies claimed that a more intrinsic crystallization barrier and the influence of fluid chemistry (e.g., relative size of the cations in solution) may prevent the formation of long-range ordered crystallographic structures in dolomite at ambient conditions (3-5). Lippmann (18) described specific superstructures, called ordering-reflections, in the X-ray diffraction patterns of dolomite that were related to the regular alternation of monolayers of Ca and Mg oriented perpendicular to the c-axis of dolomite crystals. This organization indicates an equal Mg and Ca composition in the structure at the crystal scale. In natural dolomites, structural imperfections are frequently measured and, sometimes, nanometer sized crystallites with short-range order may be expected (1). In this last case, the term disordered dolomite (also called protodolomite) is used because the superstructures ordering reflections, corresponding to the peaks

(101), (015) and (021)) in X-ray diffraction patterns, are not detected (13, 19).

The present study demonstrates that an amorphous calcium-magnesium carbonate phase (ACMC) accelerates the dolomitization process at room temperature under abiotic conditions. Herein, an ACMC phase was instantaneously precipitated by using concentrated ionic solutions ($HCO_3^-/CO_3^{2-}$ solution – $Mg^{2+}/Ca^{2+}$ solution interactions). Then, the persistence time or lifetime (i.e. the duration until ACMC starts transforming) and transformation of ACMC into new minerals in the interacting solutions were monitored in real-time by using dynamic Raman spectroscopy (20). We also investigated the effect of the Mg molar fraction with respect to Ca in solution. This parameter controls the amount of Mg that can be incorporated into the carbonate crystal lattice and the nature of transient carbonate phases, allowing to the precipitation of calcite (Mg/(Mg+Ca) = 0), low Mg-calcite (Mg/(Mg+Ca)<10%), high Mg-calcite (10%<Mg/(Mg+Ca)<45%), disordered dolomite (45%<Mg/(Mg+Ca)≤55%) and high Ca-magnesite (Mg/(Mg+Ca)>60%), as reported in the literature (e.g. 21-25).

High Mg-calcite and disordered dolomite precipitation at room temperature is frequently related to bio-mineralization processes, as observed in corals, seashells and many other invertebrates or observed in laboratory experiments under biotic conditions (16, 21). The present experimental study demonstrates that disordered dolomite, $CaMg(CO_3)_2$, can precipitate at low temperature when ideal Mg/Ca ratio, high-carbonate alkalinity ($HCO_3^-/CO_3^{2-}$ coexistence) and high ionic-concentration are reached in abiotic or biotic systems. Herein, the formation of an amorphous phase plays a significant role to produce disordered dolomite

## 2. Materials and Methods

### *2.1. Disordered dolomite $CaMg(CO_3)_2$ formation at room temperature*

The conditions to precipitate disordered dolomite at room temperature (27-31°C) were the following: 100 mL of $NaHCO_3$ (1M) and 100 mL of $Na_2CO_3$ (1M) were placed into a Hastelloy C22 reactor (Parr, total internal volume of 600 mL) coupled with a Raman probe immerged into solution/suspension in order to monitor in real-time precipitating carbonate particles and aqueous carbonate species. This experimental setup was reported previously in Montes-Hernandez group (20). Raman spectra were collected with a Raman RXN1, Kaiser Optical Systems with an exposure time of three seconds and averaged over three scans.

The carbonate speciation in initial solution was verified by Raman spectroscopy before the injection of Ca-Mg solution ($HCO_3^-$ peaking at 1016 $cm^{-1}$ and $CO_3^{-2}$ peaking at 1066 $cm^{-1}$; see Fig. S1-A). This carbonate alkaline solution was immediately dispersed by mechanical agitation (400 rpm) before 200 ml of a Ca-Mg solution (Mg molar fraction of 0.75 and Mg concentration of 0.375M) were injected for about 1-2 minutes with a syringe. Following this injection step, the carbonate speciation and precipitated particles (i.e. transformation of amorphous calcium-magnesium carbonate ACMC into carbonate crystalline phases) were monitored by Raman spectroscopy for three to seven days, with an acquisition frequency of one Raman spectra every minute during the first three hours and every five or ten minutes in the remaining time.

Selected Raman peaks corresponding to identified mineral phases (see Table S1) were fitted by using simple or combined Gaussian model in order to estimate both the full wide half maximum (FWHM) and integrated peak area as a function of time (Movie S1). This calculation provided the

peak decomposition necessary to propose relevant reaction mechanisms and to quantify the kinetics of precipitation of disordered dolomite ($MgCa(CO_3)_2$).

### *2.2. Role of Mg molar fraction*

The persistence time of amorphous calcium magnesium carbonate (ACMC) and its transformation into crystalline carbonate phases in the interacting solutions were measured as a function of Mg molar fraction (Mg molar fraction = $(V_{Mg}/(V_{Mg}+V_{Ca}))$ that was varied between 0 and 1 (experiments 5-11 in Table 1). Herein, the persistence time, also called lifetime, is defined as the duration over which ACMC is the only precipitate phase present in the suspension before starting to transform into crystalline carbonate phases. We define the nucleation time of each crystalline phase as the time where this mineral is detected by Raman spectroscopy. These experiments were performed following the same protocol described in section 2.1, except for the added volume of Ca and Mg solutions that was adjusted for each investigated Mg molar fraction. Table 1 summarizes all precipitation experiments performed in this study; each experiment was repeated at least twice to verify reproducibility of the results.

### *2.3. Ex situ characterization of precipitates*

At the end of each experiment, the solid product was recovered by centrifugation and washed twice with ultrapure water, and once with ethanol. Then, it was dried under a laminar flow of air at 20°C for 48 h. The dry solid products were stored in plastic flasks for subsequent characterization of selected samples by Field Emission Gun Scanning Electron Microscopy (FESEM), Transmission Electron Microscopy (TEM) and powder X-ray diffraction (XRD).

Powder XRD spectra were acquired using a Siemens D5000 diffractometer in Bragg-Brentano

geometry, equipped with a theta-theta goniometer with a rotating sample holder. Diffraction patterns were collected using Cu k$\alpha_1$ ($\lambda_{k\alpha1}$=1.5406 Å) and Cu k$\alpha_2$ ($\lambda_{k\alpha2}$=1.5444 Å) radiations in the range $2\theta$ = 10 - 70°, with a step size of 0.04° and a counting time of six seconds per step. For high-resolution imaging, the solid products were dispersed by ultrasonic treatment in absolute ethanol for five minutes. Two droplets of the suspension were then deposited directly on an aluminum support and coated with gold-platinum. The powder was imaged using a Zeiss Ultra 55 FESEM with a maximum spatial resolution of approximately 1 nm at 15kV. In addition, recovered solid products from experiments 1 and 2 (Table 1) were shaken in ethanol for a short time in order to separate the aggregates without any additional treatment. One droplet of the suspension was deposited on a perforated carbon foil and placed on a conventional copper micro-grid for further observations with a JEOL 2100F Transmission Electron Microscope (TEM) operating at 200 kV, equipped with a field emission gun and a high-resolution pole piece achieving a point-to-point resolution of 1.8 Å. Chemical analyses in selected points on the sample were performed by Electron Dispersive Spectroscopy (EDS).

## 3. Results

### *3.1. Precipitation of disordered dolomite at room temperature: Reaction mechanism and kinetics*

Concentrated ionic solutions were chosen to produce an amorphous calcium-magnesium carbonate (ACMC) phase. Our in-situ Raman spectroscopy data confirmed the instantaneous formation of ACMC when alkaline carbonate solution ($HCO_3^-/CO_3^{-2}$=1) was mixed with Mg-Ca solution (Mg molar fraction = 0.75), as displayed for three experiments in Fig. S1-B. The precipitated ACMC ($Ca_{0.5}Mg_{0.5}CO_3.nH_2O$) is characterized by a broad Raman peak at 1085 $cm^{-1}$, shifted 6 $cm^{-1}$ away

and broader with respect to the peak of amorphous calcium carbonate (ACC: $CaCO_3.nH_2O$) at 1079 $cm^{-1}$ (this study), close to the value of 1080 $cm^{-1}$ reported in other studies (e.g. 26-27). Time-resolved Raman spectroscopy shows that ACMC starts transforming into crystalline phases after about 2.5 h of reaction. Nesquehonite ($MgCO_3.3H_2O$) is the first detected phase, with a peak at 1099 $cm^{-1}$ and a nucleation time of 2.5 h, followed by monohydrocalcite ($CaCO_3.H_2O$), with a peak at 1067 $cm^{-1}$ and a nucleation time of 3.3 h (Fig. 1). All phases detected in the time-resolved Raman spectroscopy measurements are summarized in Table S1 and their Raman feature assignation is supported by previous studies that used systematically ex-situ Raman spectroscopy onto powdered samples. Nesquehonite and monohydrocalcite are transient phases, i.e. their slow concurrent dissolution allows the continuous precipitation of disordered dolomite with a Raman peak at 1094 $cm^{-1}$ (Fig. 2). Broad feature of the main peak and low Raman signal in lattice mode at 300 $cm^{-1}$ suggest the presence of nanosized crystals, as confirmed by FESEM images that reveal crystallites with size in the range 20 to 80 nm and forming irregular aggregates (Fig. S2). Herein, we suggest that this phase is a disordered dolomite, i.e. short-range order forming nanosized crystallites, because the superstructures ordering reflections ((101), (015) and (021)) are not detected in our laboratory X-ray powdered diffraction, despite an ideal atomic composition (Mg/Ca=1) (Fig. S3). The movie S1 displays the time evolution of the peaks of the main mineral phases during experiment 2 (Table 1), leading to the formation of disordered dolomite, including the evolution of ACMC, nesquehonite, and monohydrocalcite. The surface areas of the peaks corresponding to these four phases evolve as a function of time and are used here as proxies to measure the relative concentrations of these components in the suspension (Fig. S4).

From these time-resolved Raman measurements and spectra analyses (Figs. 1, 2 and S4), the following reactions are proposed, which summarize the mechanism for disordered dolomite

175 formation:

176 **Nesquehonite formation**

177 $2Ca_{0.5}Mg_{0.5}CO_3.nH_2O + 3H_2O \rightarrow MgCO_3.3H_2O + CaCO_3.nH_2O + nH_2O$ (1)

178 **Monohydrocalcite formation**

179 $CaCO_3.nH_2O + H_2O \rightarrow CaCO_3.H_2O + nH_2O$ (2)

180 **Formation of disordered dolomite via concurrent dissolution of transient phases**

181 $MgCO_3.3H_2O + CaCO_3.H_2O \rightarrow CaMg(CO_3)_2 + 4H_2O$ (3)

182 Data show that the concurrent slow dissolution of nesquehonite and monohydrocalcite nourish the
183 precipitation of disordered dolomite. However, disordered dolomite nucleation formed during the
184 first hours (nucleation time = 3.2h), as detected by fitting the Raman spectra (see Movie S1 and
185 Fig. S4). These results imply that nesquehonite and monohydrocalcite play a critical retarding
186 effect on the formation of disordered dolomite as discussed below.

187 The precipitation of disordered dolomite from direct transformation of ACMC could also occur as:

188 $2Ca_{0.5}Mg_{0.5}CO_3.nH_2O \rightarrow CaMg(CO_3)_2 + 2nH_2O$ (4)

189 This more simple reaction mechanism was detected by time-resolved Raman spectroscopy (Fig. 3,
190 experiment 1 in Table 1), but with a low experimental reproducibility (once over four total
191 experiments performed under identical conditions, experiments 1 to 4 in Table 1). In this particular
192 case, the lifetime of ACMC was larger and equal to 10 hours, as shown on Fig. 3. Herein, the
193 particle size distribution of disordered dolomite was more homogeneous with an average size of
194 20 nm (see FESEM images in Fig. S2 for experiment 1). We assumed that, in this particular case,
195 ACMC reached an ideal Mg/Ca ~ 1 ratio and then its direct transformation into disordered dolomite
196 could take place, as demonstrated by the Raman data (Fig. 3). However, this chemical event might
197 be strongly sensitive to small fluctuations of room temperature, fluid chemistry, mechanical

198 agitation and time of mixture of ionic solutions because it happened only once over the four
199 experiments performed under the same conditions (experiments 1-4 in Table 1).
200 In natural open systems oversaturated with respect to dolomite, fluid chemistry and temperature
201 fluctuations could inhibit dolomite formation and the precipitated transient phases could remain
202 persistent and stable for long durations (e.g. 28-29). Such observations may provide an explanation
203 why dolomite is absent in natural systems presently oversaturated with respect to dolomite.
204
205 *3.2. Role of Mg molar fraction*
206 At the investigated carbonate alkaline conditions ($HCO_3^-/CO_3^{2-}$ = 1, 0.5 M for each specie, and
207 pH~$pK_{a2}$~10.3), both the concentration of Mg and its molar fraction with respect to Ca play a
208 critical role on the lifetime of ACMC. When the Mg molar fraction is larger than 0.5, the ACMC
209 lifetime increases substantially (Fig. 4). The reaction mechanism, i.e. the nature of transient
210 crystalline phases and final recovered products, is also strongly dependent on the concentration of
211 Mg (see Table 1). For example, when the Mg molar fraction is less or equal than 0.2, vaterite
212 polymorph is the main transient phase before the formation of low Mg-calcite ($Mg_xCa_{1-x}CO_3$ with
213 $x<0.1$) (Fig. S5). Here, three reaction steps are clearly identified: (1) ACC formation with a lifetime
214 of 3 minutes; (2) concurrent transformation of ACC into vaterite and Mg-calcite; and (3) slow
215 transformation of vaterite into low Mg-calcite via coupled dissolution-crystallization process. This
216 reaction mechanism is in agreement with results obtained from in-situ time-resolved synchrotron-
217 based wide-angle X-ray scattering (WAXS) and energy dispersive X-ray diffraction (ED-XRD),
218 despite the difference in pH and Mg concentration (30). At higher Mg molar fraction (e.g. 0.5 and
219 0.6), high Mg-calcite mesocrystals ($Mg_xCa_{1-x}CO_3$ with $0.1<x<0.45$) form and the vaterite phase is
220 not detected (see Table 1). Mg-calcite mesocrystals are micrometric porous aggregates constituted

of oriented nano-crystals and that form cauliflower and peanut-like morphologies (Fig. S6). These peculiar morphologies and the process of aggregation of nanocrystals have been reported in previous studies (e.g. 22-23). In some studies, high-Mg calcite with peculiar morphologies and with Mg content into crystal lattice (<45%) was misinterpreted as disordered dolomite (e.g. 15-16). Therefore, Mg-calcite mesocrystals are not necessary made of disordered dolomite, except when the Mg/Ca ratio of the crystal lattice is close to 1.

At a Mg molar fraction of 0.75 and under abiotic conditions, we observed the formation of disordered dolomite ($CaMg(CO_3)_2$), as discussed in section 3.1. In complement, X-ray data (Fig. 5) show the (104) reflection in the solid products recovered at the end of experiments that used different initial Mg molar fraction (see also Table 1. In addition, from Rietveld refinements of XRD patterns, the Table 2 summarizes the mineral composition and Mg content into calcite crystal lattice. In general, our results are in agreement with studies that have investigated the influence of Mg molar fraction on the lifetime of ACC and ACMC phases and their transformation into crystalline phases (e.g. 28-30). In addition to already published studies, our study reports specific experimental conditions that allow the synthesis of disordered dolomite by controlling exclusively the Mg molar content (0.75) and the carbonate alkalinity ($HCO_3^-/CO_3^{2-}$=1, pH~$pK_{a2}$~10.3) at room temperature (experiments 1-4 in Table 1).

Finally, for Mg molar fraction of 0.9 (experiment 10 in Table 1), the lifetime of ACMC was prolonged to about 4.5 hours and a more complex reaction mechanism was monitored by time-resolved Raman spectroscopy (Fig. 6). In this experiment, monohydrocalcite ($CaCO_3 \cdot H_2O$) was detected as a transient phase before the formation of disordered dolomite and high Ca-Magnesite was measured by X-ray diffraction in the product recovered after the experiment (Fig. 5 and Table

2). Dypingite ($Mg_5(CO_3)_4(OH)_2 \cdot 5H_2O$) was also detected, and this hydrated carbonate co-existed with disordered dolomite and Ca-magnesite until the end of experiment (Fig. 6). These results demonstrate that the Mg molar fraction controlled the lifetime of ACMC in the interacting solutions, the reaction mechanism, the kinetics, and the amount of Mg incorporated into the carbonate.

## 4. Discussion and concluding remarks

Dolomite is a critical mineral that incorporates large volumes of carbon dioxide into a solid form in many geological environments (1). Primary dolomite formation ($Mg^{2+} + Ca^{2+} + 2CO_3^{2-} \rightarrow CaMg(CO_3)_2$) at low temperature (20-35°C) and secondary dolomite formation ($2CaCO_3 + Mg^{2+} \rightarrow CaMg(CO_3)_2 + Ca^{2+}$) at higher temperature (diagenetic or hydrothermal, 60-300°C) have been proposed to explain dolomitization processes in natural environments (1). Primary dolomite formation has led to controversial claims because ordered dolomite could not be synthesized in laboratory under abiotic conditions and only disordered dolomite and high Mg-calcite are generally observed in environments oversaturated with respect to dolomite (2, 15-17). Bio-assisted primary dolomite formation, and/or formation mediated by living organisms, have been proposed. In such cases, cellular and intracellular surfaces and exopolymeric substances can overcome the kinetic barrier to nucleate dolomite (e.g. 6-12). Functionalized organic molecules/surfaces can also decrease the Mg hydration barrier and catalyze dolomite formation at low temperature (e.g. 31). However, the reaction mechanism responsible for dolomite formation (e.g., role of transient amorphous or crystalline phases) and clear proofs or explanations concerning the dolomite superstructures ordering reflections in the X-ray diffraction patterns have been ambiguously provided (6, 12). Based on the present study and on recent mechanisms proposed to explain mineral

nucleation (e.g. 32-36), we infer that primary dolomite, as initially defined ($Mg^{2+} + Ca^{2+} + 2CO_3^{2-} \rightarrow CaMg(CO_3)_2$), has a very low probability to form at room temperature in abiotic or biotic systems, i.e. through heterogeneous nucleation (pre-existence of reactive surfaces) and a non-classical nucleation mechanism is therefore expected. The present study demonstrates that transient amorphous or crystalline phases play a significant role in the formation of disordered dolomite. Such transient phases can decrease the energy barrier under ideal fluid chemistry conditions (e.g. direct transformation of ACMC into disordered dolomite), but, they can also retard dolomite precipitation (e.g. via concurrent dissolution of nesquehonite and monohydrocalcite) as demonstrated in the present study (Figs. 1, 2, 3 and movie S1). Crystalline phases (e.g. dypingite, monohydrocalcite, aragonite) can produce an inhibiting effect in laboratory experiments or in some natural dolomitic environments (1). From the present experimental study, we conclude that ACMC accelerates dolomitization in a short interval of Mg molar content (0.6-0.75) at low temperature and the revealed reaction mechanism could exist in natural dolomitic environments such as lagoons, evaporitic settings, or caves.

Another critical point concerning the so-called primary dolomite is the existence of superstructures ordering reflections in X-ray diffraction patterns (e.g. (101), (015) and (021), Fig. S3). Herein, some factors can perturb their unambiguous detection. For example, when dolomite crystal size is larger than 100 nm and coexisting crystalline phases have a low concentration, X-ray powder diffraction or electron diffraction in TEM allow a clear identification of superstructure ordering reflections. Conversely, if dolomite crystal size is of the order or smaller than 20 nm (Fig. S7), the detection of superstructure ordering reflections is more challenging in X-ray diffraction patterns and by electron diffraction in TEM when nanoparticles are aggregated, despite the ideal Mg content (Ca/Mg ~1) in the structure lattice (Fig. S3). In such case, disordered dolomite, i.e. short-range

ordered crystallographic structures, is assumed and in general, longer range ordering is reached with an increase of temperature (corresponding to an increase of average size of dolomite crystals) as already demonstrated in a previous study (13). We claim that the detection limit of laboratory X-ray diffraction data when nanoparticles exist (the peaks are broader and have lower intensity and the low intensity of superstructure ordering reflections) and the difficulty to synthesize dolomite in laboratory experiments have led to contradictory interpretations on the formation of dolomite at low temperature. In this perspective, the formation of disordered dolomite at low temperature in abiotic systems can be achieved at room temperature. A future challenge would be to determine whether a regular alternation of monolayers of Ca and Mg (perpendicular to the c-axis) may exist in nanosized dolomitic crystals, that would require to develop specific analytical and imaging methods, such as energy filtered transmission electron microscopy combined with electron energy loss spectroscopy.

## Acknowledgements

The authors acknowledge funding from the French National Centre for Scientific Research (CNRS).

## Appendix A. Supplementary data

Supplementary material (1 Table, 7 additional figures and a spectral movie) related to this article can be found, in the online version, at

## References


(1) Warren, J. Dolomite: occurrence, evolution and economically important associations. *Earth Sci. Reviews* **2000**, 52, 1-81.

(2) Deelman, J. C. Breaking Ostwald's rule. *Chemie Der Erde-Geochemistry* **2001**, 61, 224-235.

(3) Pimentel, C.; Pina, C. M. The formation of the dolomite-analogue norsethite: Reaction pathway and cation ordering. *Geochim. Cosmochim. Acta* **2014**, 142, 217-223.

(4) Hänchen, M.; Prigiobbe, V.; Baciocchi, R.; Mazzotti, M. Precipitation in the Mg-carbonate system-effects of temperature and $CO_2$ pressure. *Chem. Eng. Sci.* **2008**, 63, 1012-1028.

(5) Xu, J.; Yan, C.; Zhang, F.; Konishi, H.; Xu, H.; Teng, H. Testing the cation-hydration effect on the crystallization of Ca-Mg-$CO_3$ systems. *Proc. Natl. Acad. Sci*. **2013**, doi: 10.1073/pnas.1307612110.

(6) Vasconcelos, C.; McKenzie, J. A.; Bernasconi, S.; Grujic, D.; Tien, A. J. Microbial mediation as a possible mechanism for natural dolomite formation at low temperatures. *Nature* **1995**, 377, 220-222.

(7) Warthmann, R.; Van Lith, Y.; Vasconcelos, C.; Mckenzie, J. A.,; Karpoff, A. M. Bacterially induced dolomite precipitation in anoxic culture experiments. *Geology* **2000**, 28, 1091-1094.

(8) Sanchez-Roman, M.; McKenzie, J. A.; Wagener, A-de-L. R.; Rivadeneyra, M. A.; Vasconcelos, C. Presence of sulfate does not inhibit low-temperature dolomite

precipitation. *Earth Planet. Sci. Lett.* **2009**, 285, 131-139.

(9) Kenward, P. A.; Goldstein, R. H.; Gonzalez, L. A.; Roberts, J. A. Precipitation of low-temperature dolomite from anaerobic microbial consortium: the role of methanogenic Archea. *Geobiology* **2009**, 7, 556-565.

(10) Deng, S.; Dong, H.; Lv, G.; Jiang, H.; Yu, B.; Bishop, M. E. Microbial dolomite precipitation using sulfate reducing and halophilic bacteria: Results from Qinghai lake, Tibetan Plateau, NW China. *Chem. Geol.* **2010**, 278, 151-159.

(11) Krause, S.; Liebetrau, V.; Gorb, S.; Sanchez-Roman, M.; Mackenzie, J. A.; Treude, T. Microbial nucleation of Mg-rich dolomite in exopolymeric substances under anoxic modern seawater salinity: New insight into an old enigma. *Geology* **2012**, 40, 587-590.

(12) Daye, M.; Higgins, J.; Bosak, T. Formation of ordered dolomite in anaerobic photosynthetic biofilms. *Geology* **2019**, 47, 510-512.

(13) Montes-Hernandez, G.; Findling, N.; Renard, F. Dissolution-precipitation reactions controlling fast formation of dolomite under hydrothermal conditions. *App. Geochem.* **2016**, 73, 169-177.

(14) Vandeginste, V.; Snell, O.; Hall, M. R.; Steer, E.; Vandeginste, A. Acceleration of dolomitization by zinc in saline waters. *Nature Communications* **2019** doi.org/10.1038/s41467-019-09870-y

(15) Liu, D.; Xu, Y.; Papineau, D.; Yu, N.; Fan, Q.; Qiu, X.; Wang H. Experimental evidence for abiotic formation of low-temperature proto-dolomite facilitated by clay

minerals. *Geochim. Cosmochim. Acta* **2019**, 247, 83-95.

(16) Huang, Y.-R.; Yao, Q.-Z.; Lia, H.; Wang, F.-P.; Zhou, G.-T.; Fu, S.-Q. Aerobically incubated bacterial biomass-promoted formation of disordered dolomite and implication for dolomite formation. *Chem. Geol.* **2019**, 523, 19-30.

(17) Qiu, X.; Wang, H.; Yao, Y.; Duan, Y. High salinity facilitates dolomite precipitation mediated by Haloferax volcaniiDS52. *Earth Planet. Sci. Letters* **2017**, 472, 197-205.

(18) Lippmann, F., 1973. Sedimentary carbonate minerals. Springer-Verlag, 228pp.

(19) Montes-Hernandez, G.; Findling, N.; Renard, F.; Auzende, A.-L. Precipitation of ordered dolomite via simultaneous dissolution of calcite and magnesite : New experimental insights into an old precipitation enigma, *Cryst. Growth Des.* **2014**, 14, 671-677.

(20) Montes-Hernandez, G.; Renard, F. Time-resolved in situ Raman spectroscopy of the nucleation and growth of siderite, magnesite and calcite and their precursors. *Cryst. Growth Des.* **2016**, 16, 7218-7230.

(21) Long, X.; Ma, Y.; Qi, L. Biogenic and synthetic high magnesium calcite – A review. *J. Struc. Bio.* **2014**, 185, 1-14.

(22) Yu, P. T.; Tsao, C.; Wang, C. C.; Chang, C. Y.; Chan, C. C. High-Magnesium Calcite Mesocrystals: Formation in Aqueous Solution under Ambient Conditions. *Angewandte Chemie Int.* **2017**. 51, 16420-16424, doi.org/10.1002/anie.201708507.

(23) Landers, J. J. M.; Dey, A.; Bomans, P. H. H.; Spielmann, J.; Hendrix, M. M. R. M.; de With, G.; Meldrum, F. C.; Harder, S.; Sommerdijk N. A. J. M. High-Magnesian Calcite

392 Mesocrystals: A Coordination Chemistry Approach. *J. Am. Chem. Soc.* **2012**, 134, 1367-
393 1373.

394 (24) Yang, H.; Chai, S.; Zhang, Y.; Ma, Y. A study on the influence of sodium carbonate
395 concentration on the synthesis of high Mg calcites. *CrystEngComm* **2016**, 18, 157-163.

396 (25) Romaneck, C.; Jimenez-Lopez, C.; Rodriguez-Navarro, A.; Sanchez-Roman, M.;
397 Sahai N.; Coleman, M. Inorganic synthesis of Fe–Ca–Mg carbonates at low temperature.
398 *Geochim. Cosmochim. Acta* **2009**, 73, 5361-5376.

399 (26) Wehrmeister, U.; Jacob, D. E.; Soldati, A. L.; Loges, N.; Hager, T.; Hofmeister W.
400 Amorphous, nanocrystalline and crystalline calcium carbonates in biological materials. *J.*
401 *Raman Spectrosc.* **2010**, 5, 926-935, doi.org/10.1002/jrs.2835.

402 (27) Wang, D.; Hamm, L. M.; Bodnar, R. J.; Dove, P. M. Raman spectroscopic
403 characterization of the magnesium content in amorphous calcium carbonates. *J. Raman*
404 *Spectrosc.* **2012**, 43, 543-548.

405 (28) Rodriguez-Blanco, J. D.; Shaw, S. Bots, P.; Roncal-Herrero, T.; Benning, L. G. The
406 role of Mg in the crystallization of monohydrocalcite. *Geochim. Cosmochim. Acta* **2014**,
407 127, 204-220.

408 (29) Rodriguez-Blanco, J. D.; Shaw, Benning, L. G. A route for the direct crystallization
409 of dolomite. *Amer. Miner.* **2015**, 100, 1172-1181.

410 (30) Rodriguez-Blanco, J. D.; Shaw, S.; Bots, P.; Roncal-Herrero, T.; Benning, L. G. The
411 role of pH and Mg on the stability and crystallization of amorphous calcium carbonate. *J.*

412 *Alloys Compd.* **2012**, 536S, S477– S479.

413 (31) Roberts, J. A.; Kenward, P. A.; Fowle, D. A.; Golstein, R. H.; Gonzalez, L. R.;
414 Moore, D. S. Surface chemistry allows for abiotic precipitation of dolomite at low
415 temperature. *Proc. Natl. Acad. Sci.* **2013**, 110(36), 14540–14545

416 (32) Gebauer, D.; Völkel, A.; Cölfen, H. Stable prenucleation calcium carbonate
417 clusters. *Science* **2008**, 322, 1819-1822.

418 (33) Dideriksen, K.; Frandsen, C.; Bovet, N.; Wallace, A. F.; Sel, O.; Arbour, T.;
419 Navrotsky, A.; De Yoreo, J. J.; Banfield, J. F. Formation and transformation of a short range
420 ordered iron carbonate precursor. *Geochim. Cosmochim. Acta*, **2015**, 164, 94–109.

421 (34) Gower, L. B.; Tirrell, D. A. Calcium carbonate films and helices grown in solution of
422 poly (aspartate). *J. Cryst. Growth*, **1998**, 191, 153-160.

423 (35) Gebauer, D.; Kellermeier, M.; Gale, J. D.; Bergstrom, L.; Colfen, H. Pre-nucleation
424 clusters as solute precursors in crystallization. *Chem. Soc. Rev.*, **2014**, 43, 2348-2371.

425 (36) Wang, T.; Cölfen, H.; Antonietti, M. Nonclassical crystallization: Mesocrystals and
426 morphology change of $CaCO_3$ crystals in the presence of a polyelectrolyte additive. *J. Am.*
427 *Chem. Soc.* **2005**, 127, 3246-3247.

Table 1. List of experiments with time-lapse Raman spectroscopy for precipitation of disordered dolomite at room temperature and influence of Mg molar ratio. A constant carbonate alkalinity of $HCO_3^-/CO_3^{2-}$=1 (0.5M) and a total cationic (Mg-Ca) concentration of 0.5M were imposed.

| **Exp.** | **Temperature (°C)** | **Mg molar fraction** | **Exp. duration (days)** | **Lifetime of ACMC** (min. / h) | **Mineral transient phase(s)** | **Final mineral phase(s)** |
|---|---|---|---|---|---|---|
| 1 | 27 | 0.75 | 3 | 10 h | none | disordered dolomite* |
| 2 | 31 | 0.75 | 7 | 2.5 h | nesquehonite monohydrocalcite | disordered dolomite* |
| 3 | 31 | 0.75 | 7 | 2.3 h | nesquehonite monohydrocalcite | disordered dolomite |
| 4 | 30 | 0.75 | 10 | 1.9 h | nesquehonite monohydrocalcite | disordered dolomite |
| 5 | 28 | 0 | 1 | 0.75 min. | vaterite | calcite* |
| 6 | 28 | 0.05 | 1 | 1.75 min. | vaterite | calcite* |
| 7 | 29 | 0.20 | 2 | 3 min. | vaterite | low Mg-calcite* |
| 8 | 27 | 0.5 | 2 | 3 min. | none | high Mg-calcite* |
| 9 | 28 | 0.6 | 2 | 30 min. | none | high Mg-Calcite* |
| 10 | 29 | 0.9 | 2 | 4.5 h | monohydrocalcite | disordered dolomite* dypingite* |
| 11 | 28 | 1 | 3 | 2 h | none | Dypingite |

* these phases were also characterized by powder X-ray diffraction

Table 2. Mineral carbonate composition and Mg content in lattice structure identified from Rietveld refinement of X-ray diffraction patterns. In experiment 10, aragonite, dypingite and eteilite were also detected.

| Exp. | Mg molar fraction | Calcite | Low Mg-Calcite | High Mg-Calcite | Disordered Dolomite | High Ca-Magnesite |
|---|---|---|---|---|---|---|
| 5 | 0 | $CaCO_3$ | none | none | none | None |
| 6 | 0.05 | $CaCO_3$ | none | none | none | none |
| 7 | 0.20 | $CaCO_3$ | $Mg_{0.05}Ca_{0.95}CO_3$ | none | none | none |
| 8 | 0.50 | none | none | $Mg_{0.15}Ca_{0.85}CO_3$ $Mg_{0.23}Ca_{0.77}CO_3$ | none | none |
| 9 | 0.6 | none | none | $Mg_{0.35}Ca_{0.65}CO_3$ | none | none |
| 1 | 0.75 | none | none | none | $Mg_{0.49}Ca_{0.51}CO_3$ | none |
| 10 | $0.9^x$ | none | $Mg_{0.07}Ca_{0.93}CO_3$ | none | $Mg_{0.45}Ca_{0.55}CO_3$ | $Mg_{0.68}Ca_{0.32}CO_3$ |

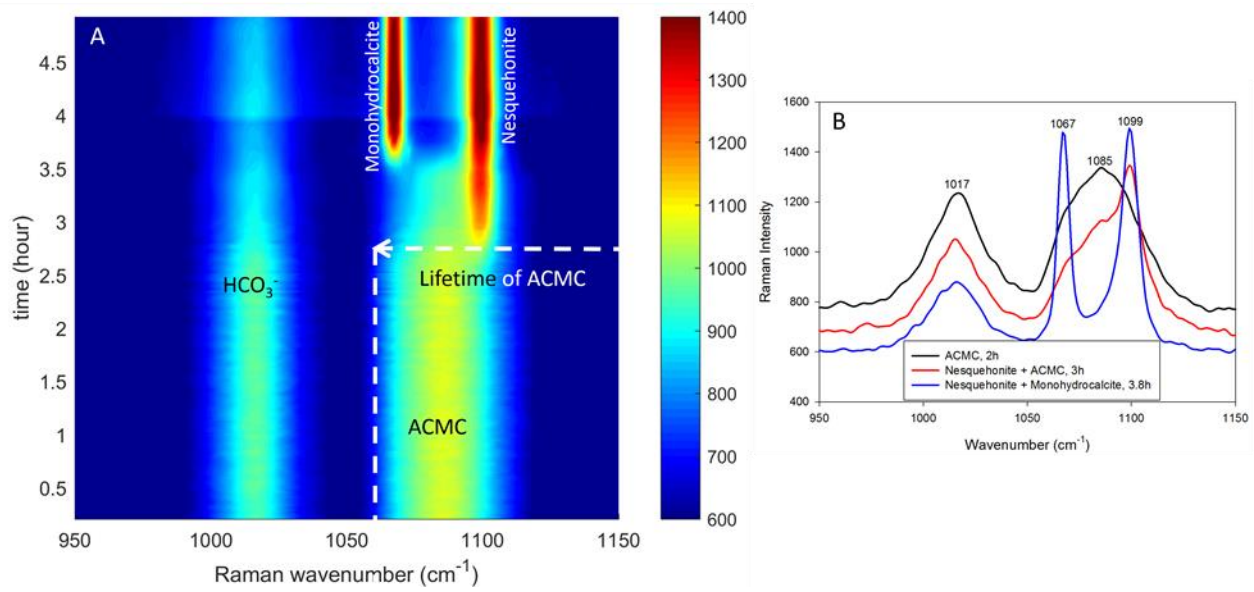


Figure 1. Time-lapse Raman spectroscopy monitoring of amorphous calcium-magnesium carbonate (ACMC) transformation into crystalline phases during the first four hours of experiment 2 (Table 1). The lifetime of ACMC and positions of crystalline phases are indicated.

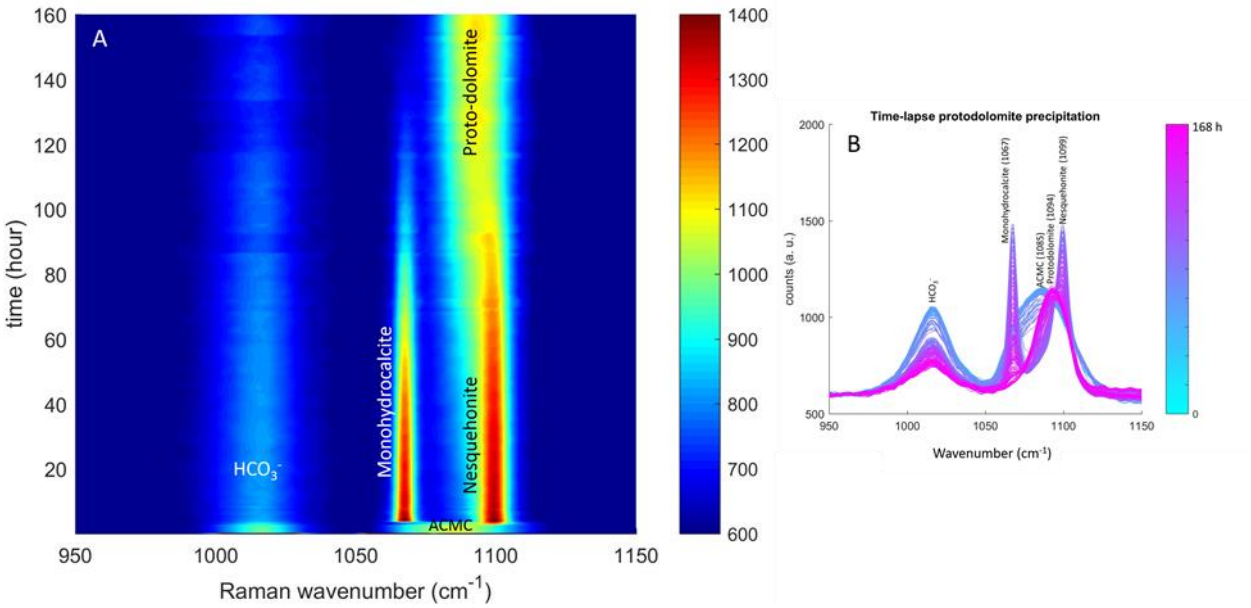


445

446

447

448

449

450

451 Figure 2. Time-lapse Raman spectroscopy monitoring of the formation of disordered dolomite from
452 ACMC in experiment 2 (Table 1). Left: evolution of the two transient phases, nesquehonite and
453 monohydrocalcite. Right: time-lapse evolution of the main peaks.

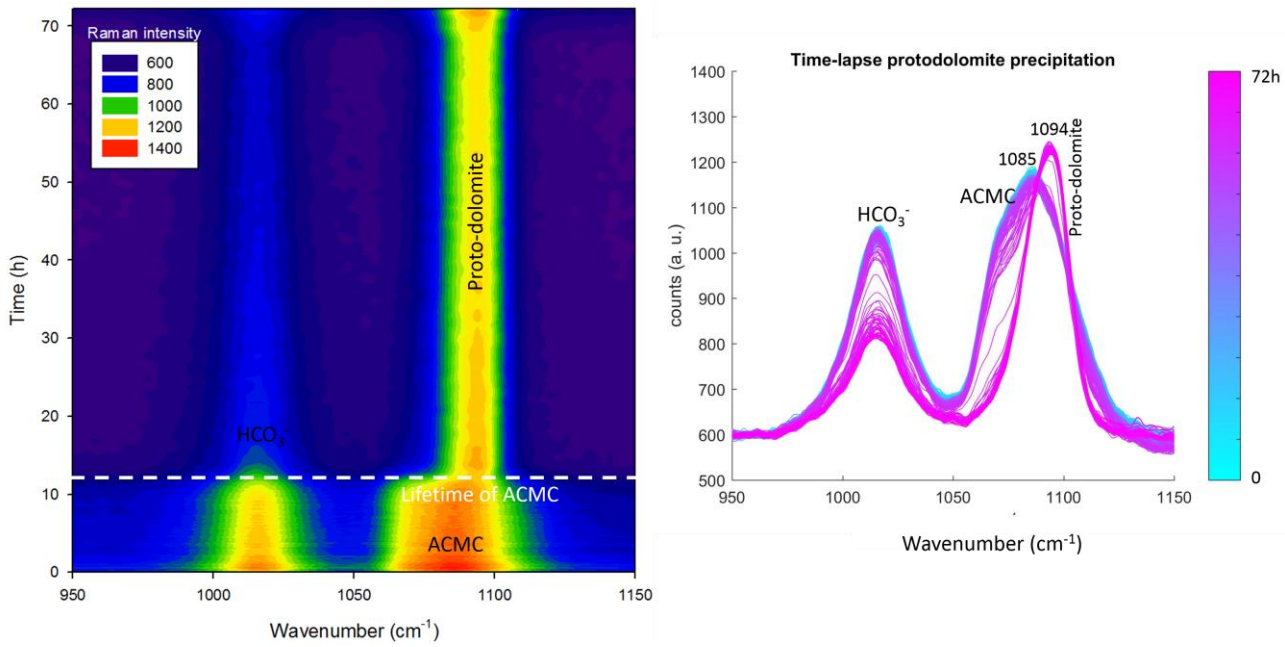


454

455 Figure 3. Left: Time-lapse Raman spectroscopy monitoring of the formation of disordered dolomite
456 from direct transformation of ACMC in experiment 1 (Table 1). Right: time-lapse evolution of the
457 main peaks.

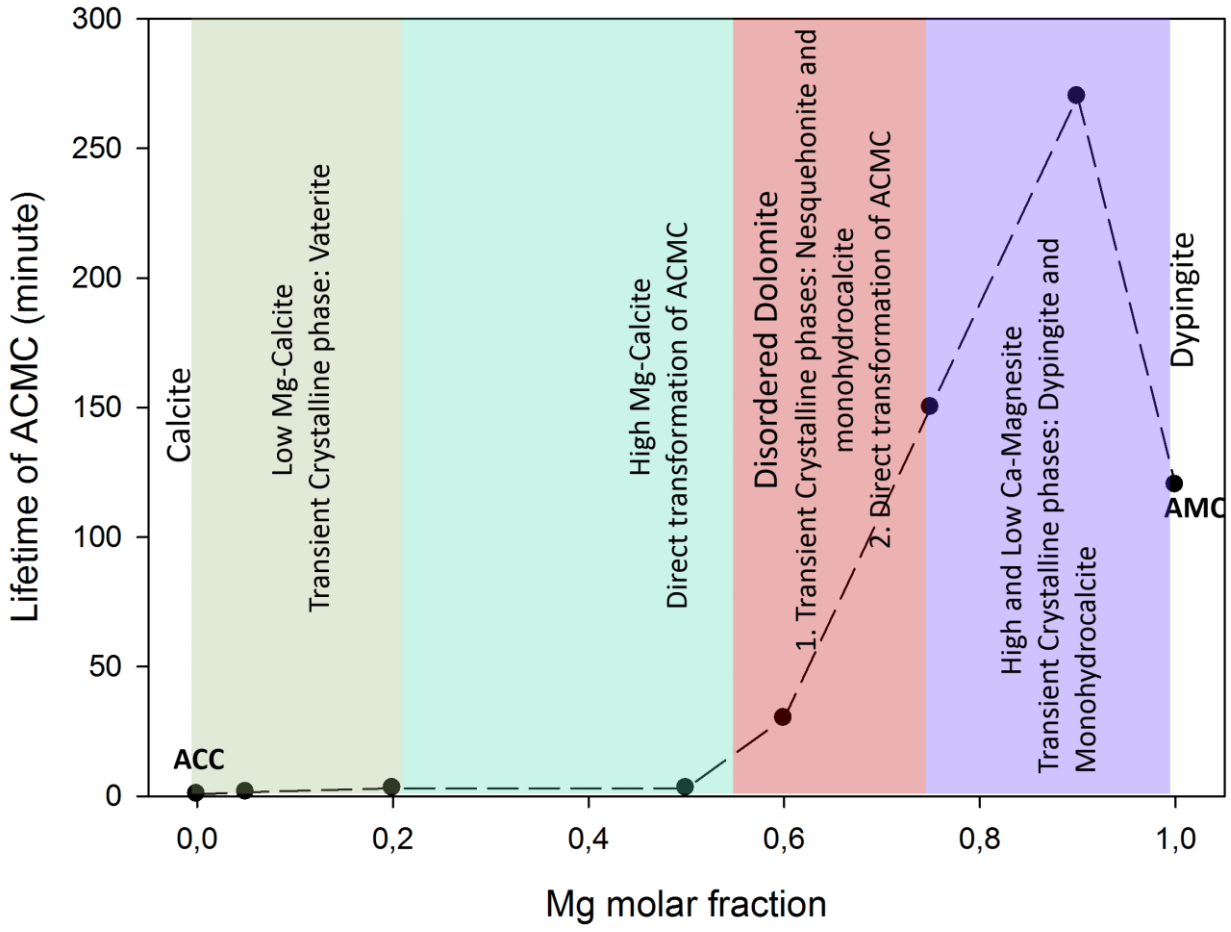


458

459 Figure 4. Lifetime of ACMC determined from time-resolved Raman measurements as a function
460 of Mg molar fraction. Eight precipitation experiments were performed with initial alkaline solution
461 ($HCO_3^-/CO_3^{2-}$ molar ratio =1, and 0.5 M) at room temperature. ACC: amorphous calcium
462 carbonate; ACMC: amorphous calcium-magnesium carbonate; AMC: amorphous magnesium
463 carbonate.

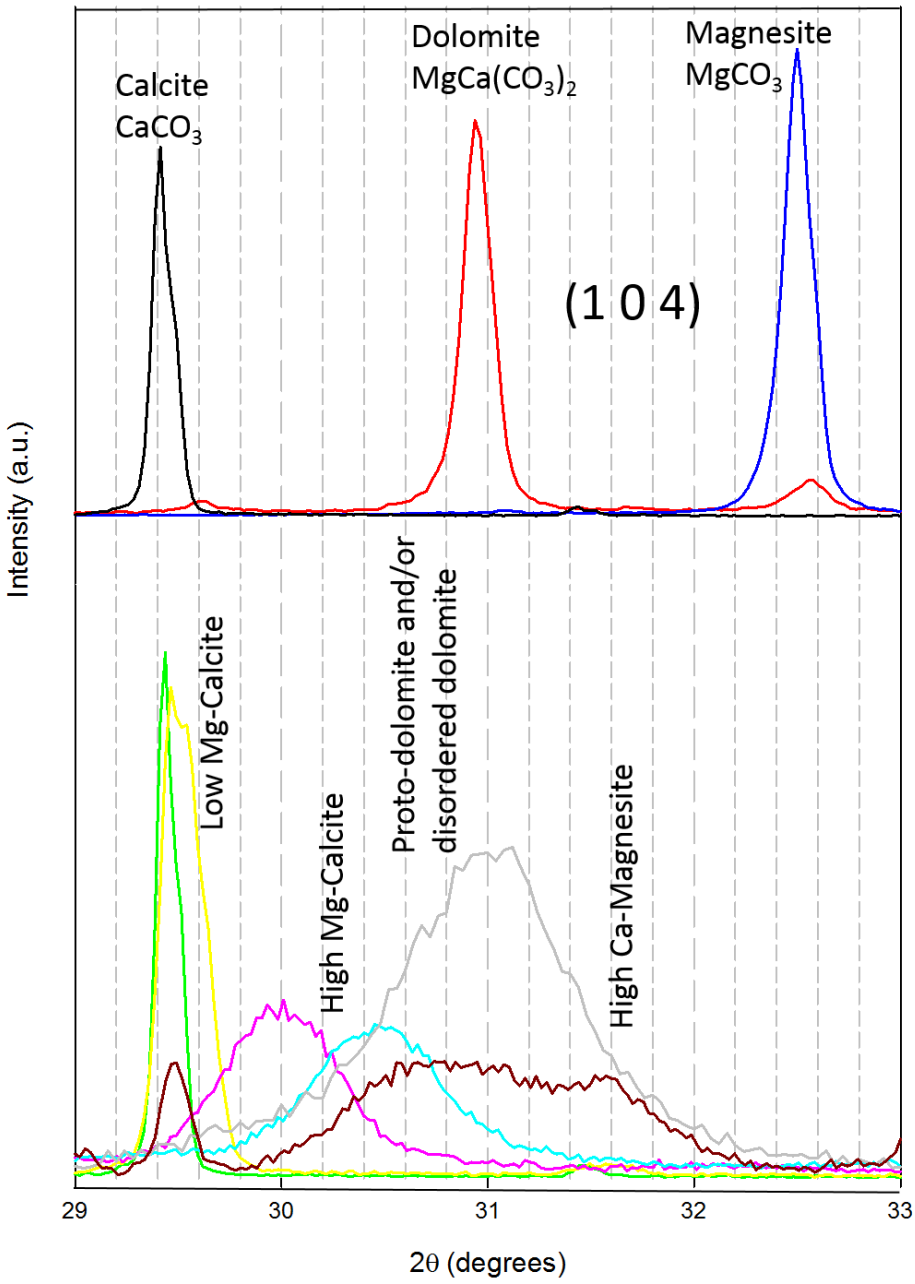


464

465 Figure 5. X-ray diffraction data showing the (104) reflection for calcite, dolomite and magnesite
466 references (13) and solids obtained for different initial Mg molar fraction in the solution: 0.05:
467 green; 0.2: yellow; 0.5: pink; 0.6: cyan; 0.75: gray; 0.9: dark red, corresponding to experiments 6-
468 10 in Table 1, respectively.

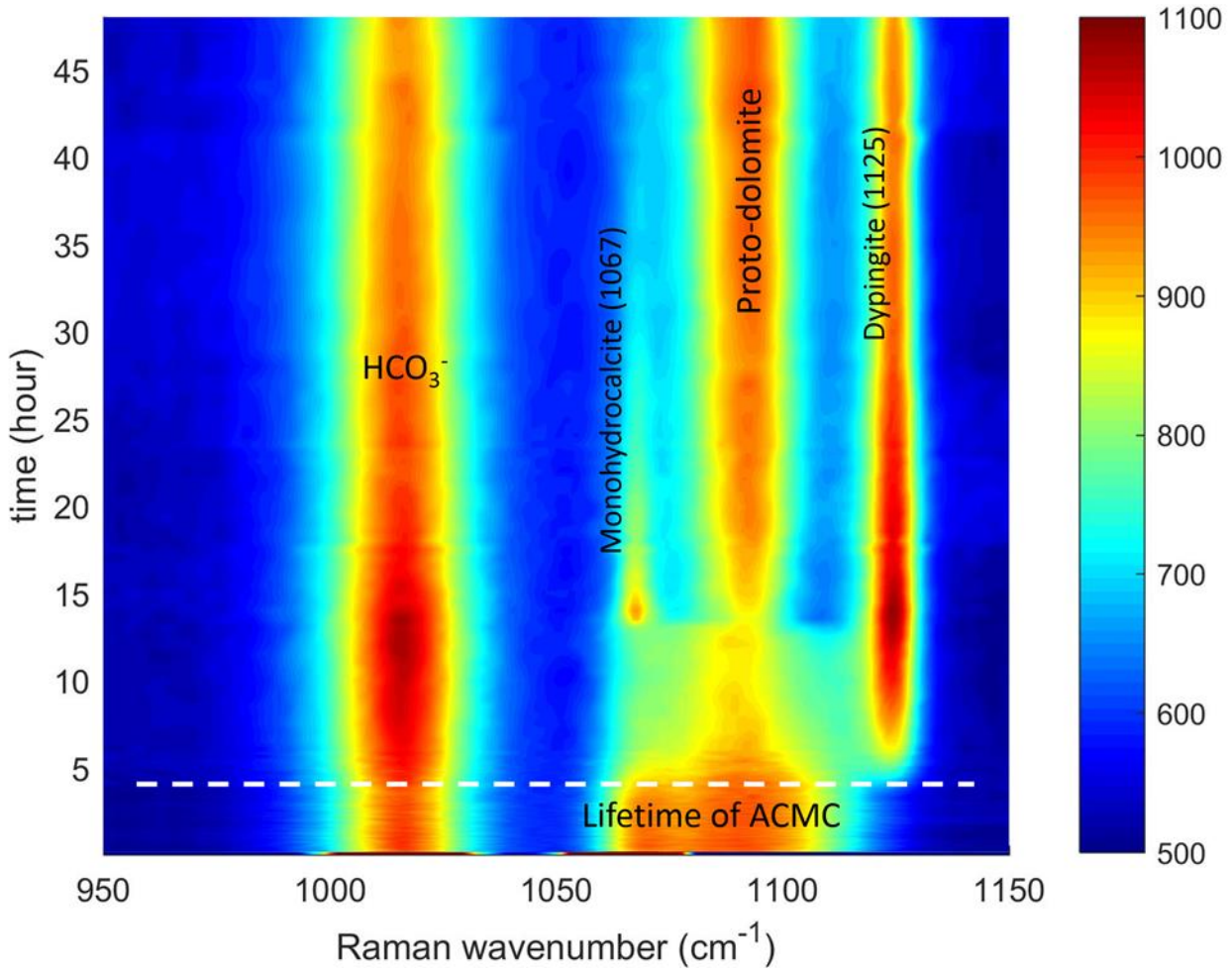


Figure 6. Time-lapse Raman spectroscopy monitoring of the formation of disordered dolomite from ACMC in experiment 10 (Table 1). Monohydrocalcite is a transient phase (Mg molar fraction of 0.9) and dypingite (hydrated Mg carbonate mineral: $Mg_5(CO_3)_4(OH)_2.5H_2O$) coexist with disordered dolomite until the end of experiment.

# Amorphous calcium-magnesium carbonate (ACMC) accelerates dolomitization at room temperature under abiotic conditions

By German Montes-Hernandez, François Renard, Anne-Line Auzende, Nathaniel Findling

## Table of Contents Graphic

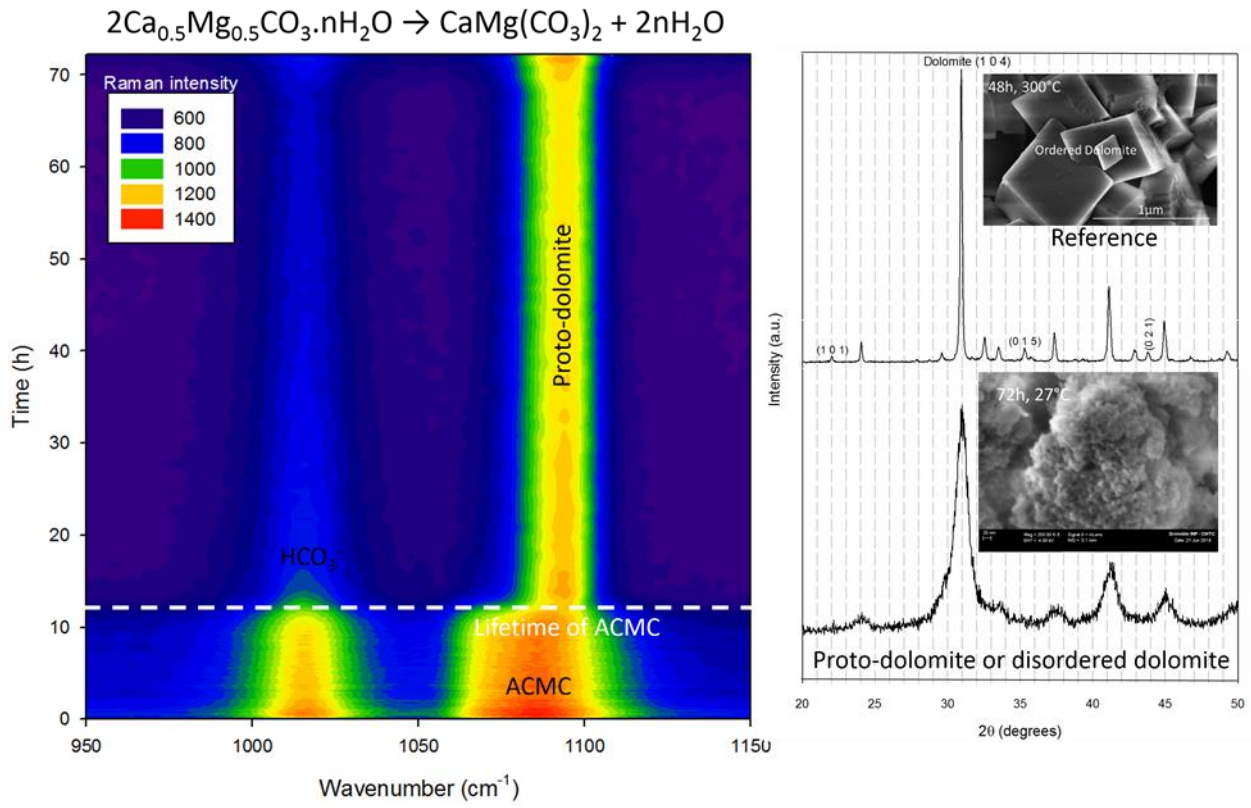


**Synopsis:** The present study reports on specific abiotic conditions that allows the precipitation of disordered dolomite, high Mg-calcite and high Ca-magnesite at room temperature over time scales of hours to days. Here we show that an amorphous calcium magnesium carbonate (ACMC) phase accelerates dolomitization at room temperature.